Energy and Buildings 41 (2009) 190–196

Contents lists available at ScienceDirect

Energy and Buildings

journal homepage: www.elsevier.com/locate/enbuild

Effect of solar chimney inclination angle on space flow pattern and ventilation rate

Ramadan Bassiouny *, Nader S.A. Korah

Department of Mechanical Power Engineering and Energy, Minia University, Minia 61111, Egypt

ARTICLE INFO

Article history:
Received 25 August 2008
Accepted 30 August 2008

Keywords:
Solar chimney
Ventilation
ACH
CFD
Inclination angle

ABSTRACT

The solar chimney is a simple and practical idea that is applied to enhance space natural ventilation. The chimney could be vertical or inclined. The chimney inclination angle is an important parameter that greatly affects space flow pattern and ventilation rate.

In the present study, the effect of chimney inclination angle on air change per hour and indoor flow pattern was numerically and analytically investigated. A numerical simulation using Ansys, a FEM-based code, was used to predict flow pattern. Then the results were compared with published experimental measurements. A FORTRAN program was developed to iteratively solve the mathematical model that was obtained through an overall energy balance on the solar chimney.

The analytical results showed that an optimum air flow rate value was achieved when the chimney inclination is between 45° and 70° for latitude of 28.4°. The numerically predicted flow pattern inside the space supports this finding. Moreover, in the present study a correlation to predict the air change per hour was developed. The correlation was tested within a solar intensity greater than or equal to 500 W/m^2, and chimney width from 0.1 m to 0.35 m for different inclination angles with acceptable values.

1. Introduction

Space air ventilation is very necessary to remove indoor pollution and dilute contamination. This ventilation can be naturally achieved based on the solar chimney principle. The driving force in the solar chimney is the buoyancy force. The solar energy absorbed by the chimney causes the air layer that exists between two, vertical or inclined, parallel plates to heat up and accordingly moves upward. As a result, it starts entraining air from the space to move towards the chimney inlet. Thus, a breeze is created inside the space allowing fresh outdoor air to enter the space through open windows or doors.

The solar chimney applications attract many researchers to sail through and discover the parameters that significantly affect its performance. Many researchers investigate the use of solar chimney, with different configurations, in natural ventilation improvement. Some have been analyzing the performance of vertical chimney under different configurations such as [1,2] while others have been studying the performance of inclined chimney.

In a study on the performance of a vertical solar chimney, Ramadan and Nader [1] concluded that increasing the chimney width from 0.1 m to 0.3 m improved the ACH by almost 25%, keeping the chimney inlet size fixed. In addition, they found out that the chimney width has a more significant effect on the space flow pattern than the chimney inlet size.

Sudaporn and Bundit [2] experimentally investigated the effect of using a vertical chimney with and without a wetted roof to enhance indoor ventilation. They reported that the solar chimney can reduce the indoor temperature by 1–3.5 °C depending on the ambient temperature and solar intensity. In addition, spraying water on a roof along with solar chimney use can further reduce indoor temperature by 2–6.2 °C.

Mathur et al. [3] experimentally compared the rate of natural ventilation due to using four different types of solar chimney. They reported that the ventilation rate increases when the absorber is inclined at 45°. In addition, the authors mentioned that inclining the absorber enhances the ventilation rate by about 15.94% due to increasing the stack height effect.

The effect of roof solar chimney inclination angle on natural ventilation was studied by Mathur et al. [4]. The authors found that the optimum absorber inclination varies from 40° to 60° with latitude ranges from 20° to 30°. Further, they reported that the air flow rate was 10% higher at an angle of 45° compared to 30° and 60°. In their results, they quoted that the highest flow rate (190 kg/h) was obtained for the 45° inclination at noon time for an air gap of 0.3 m and inlet height of 0.3 m. They presented a table for the optimum inclination angles and their corresponding latitudes. The authors, moreover, mentioned that the optimum inclination at any place varies from 40° to 60°, depending upon latitude.

* Corresponding author. Tel.: +20 016 3916415; fax: +20 086 2346674.
E-mail address: ramadan9@yahoo.com (R. Bassiouny).

0378-7788/$ – see front matter © 2008 Elsevier B.V. All rights reserved.
doi:10.1016/j.enbuild.2008.08.009

Nomenclature

A	area, m^2
ACH	air change per hour, 1/h
C_d	coefficient of discharge
C_p	specific heat, J/kg °C
d	chimney width, m
g	gravitational acceleration, m/s^2
Gr	Grashof number
h	heat-transfer coefficient, W/m^2 °C
H, H_w	room height, and window height, m
I	solar intensity, W/m^2
k	thermal conductivity, W/m °C
L	chimney length, m
Nu	Nusselt number
P	pressure, N/m^2
Pr	Prandtl number
q	heat transfer, W
Ra	Rayleigh number
T	temperature, °C
U	overall heat-transfer coefficient, W/m^2 °C
u,υ	air velocity, m/s
W	room width, m
x,y	coordinate system

Subscripts

a	ambient
c	chimney
cond	conduction
conv	convection
f	flow
g	glass
g–a	glass to air
l	loss
r	room
rw–g	radiative from wall to glass
rg–sky	radiative from glass to sky
t	total
w	wall
w–a	wall to air

Greek symbols

α	absorptivity
β	expansion factor
ρ	density, kg/m^3
τ	transmitivity
σ	Stefan–Boltzmann constant (5.67×10^{-8} W/m^2 K^4)
ε	emissivity (0.9 for glass, and 0.95 for absorber wall)
θ	inclination angle measured from the horizontal plane, deg

Sakonidou et al. [5] investigated the optimum inclination of a solar chimney for maximum air flow. They presented a mathematical model that tracks the daily extraterrestrial solar irradiation with the daily total radiation in order to estimate the glazing, air, and absorber temperatures. Further, they compared the analytical results to a CFD model. In the same article, the authors presented an empirical correlation that predicts the air exit velocity through a rectangular cross-section chimney with an equal inlet and outlet area as

$$v = C_d \frac{\rho(T_f)}{\rho(T_r)} \left[\frac{Lg(\sin(\theta))^2 (T_f - T_r)}{T_r} \right]^{1/2}$$

The results showed that both glazing and absorber temperatures increased as the chimney inclination angle decreases from 90° to 30°; however, the air exit velocity decreases. It reached its maximum value in the inclination range of 60° to 70° for a chimney length ranges from 1–12 m and chimney gap width of 0.11 m and gap depth of 0.74 m.

Tawit and Pornsawan [6] studied using a transparent roof, together with an attic room underneath, to create the driving force that induces natural ventilation in a building. They studied different chimney inclination angles and heights for a two-floor building. They depicted the flow streamlines inside the space as well as in the attic room and vertical chimney. The results showed that increasing the inclination angle of the roof from 15° to 60° improved the air change per hour (ACH). This increase further improves for a higher solar intensity and chimney height.

Using the CFD tool in analyzing fluid flow problems, Harris and Helwig [7] computationally analyzed the effect of inclination angle on the induced ventilation rate. They recorded that the optimum angle for a maximum flow rate was 67.5° from the horizontal. This gives an increase in the ventilation rate by almost 11% compared to the vertical chimney.

The previous available studies showed no detailed depiction of the indoor air velocity pattern as a result of the absorber inclination whether through flow visualization or computational prediction. Further no mathematical correlation that can predict the ventilation rate as a function of the inclination angle and other significant parameters. So, the present study aims at displaying the space air flow pattern at different chimney inclination angles through numerical visualization. In addition, the study seeks a correlation that could relate the air change per hour to the solar intensity, the absorber inclination angle, and air gap width.

2. Mathematical model

Fig. 1(a) illustrates a schematic of the physical domain, with an attached inclined chimney of length L, and width d, and angle θ. The domain considers having an open side-window (height, H_w, is 1 m), and it is at 1 m height from the floor. The considered dimensions for this domain were 3 m height by 3 m wide, and the chimney was considered 1 m long and the air gap was taken as 0.35 m.

The solar chimney is the driving element to naturally create a breeze inside a space. The glass and absorber temperatures significantly affect the flowing air temperature, and accordingly velocity. Hence, an energy balance on the chimney is carried out. This balance considers the main elements of the chimney: the glazing, the absorber, and the air in between. Some assumptions are adopted to enable solving the mathematical model. Flow through the chimney was considered: laminar, and steady-state. Energy exchange through glass, air, and absorber was treated as one-dimensional. Air entering the chimney was considered to have the same room temperature. Energy exchange between other walls in the room and the surrounding was neglected, and chimney inlet and exit areas are equal.

Applying the energy balance concept on the 1 m^2 glass wall under the aforementioned assumptions yields the following:

$$\alpha_g A_g I + h_{rw-g} A_w (T_w - T_g) = h_{conv,g-a} A_g (T_g - T_f) + \sum q_l \qquad (1)$$

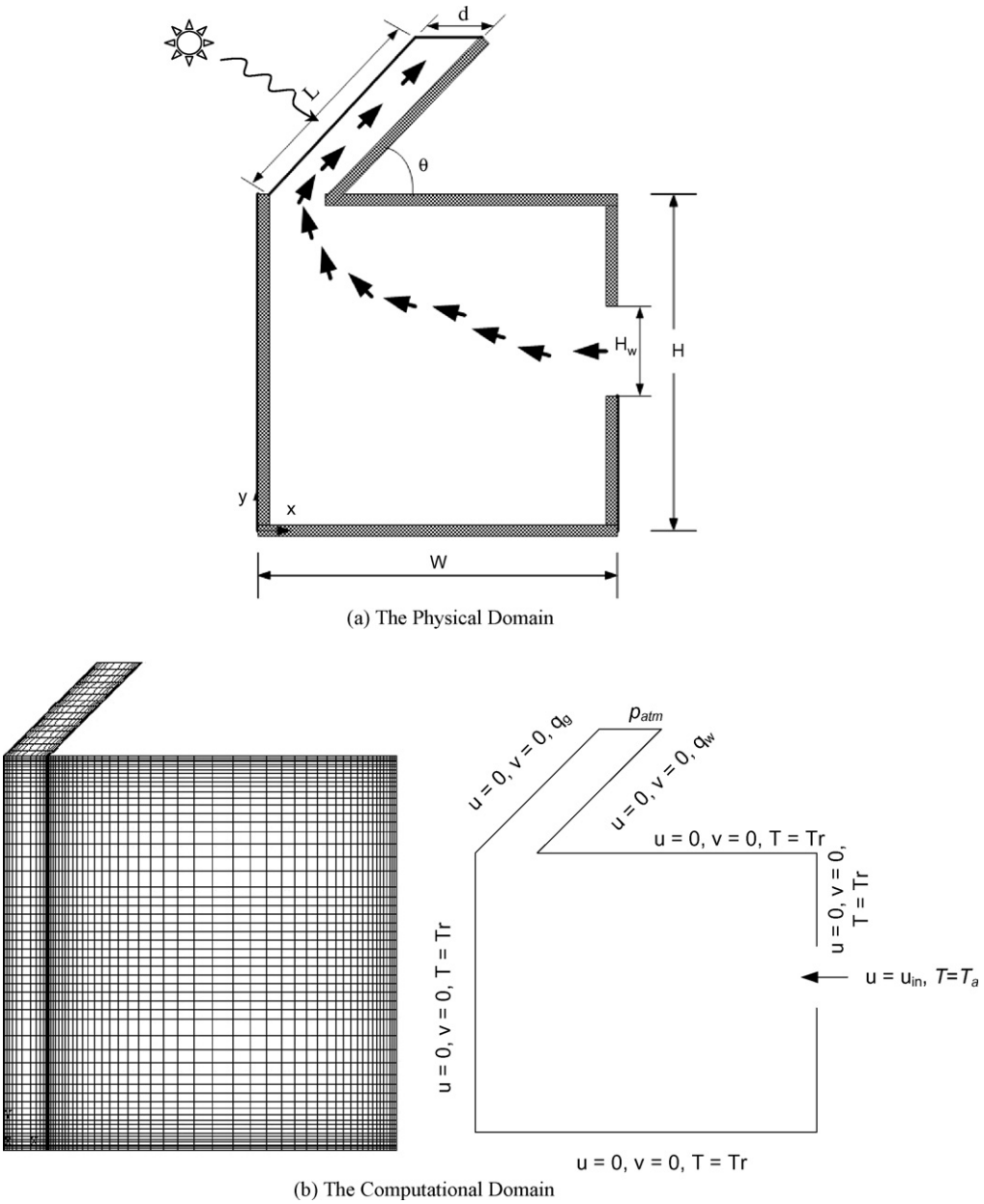

Fig. 1. The room and chimney configuration for an inclination of 45°.

The last term in the right hand side represents the losses from the glass wall to the surrounding by convection, radiation, and conduction. It can be expressed as

$$\sum q_{\mathrm{l}} = U_{\mathrm{t}} A_{\mathrm{g}} (T_{\mathrm{g}} - T_{\mathrm{a}})$$

where, U_{t} counts for the three heat-transfer coefficients as

$$U_{\mathrm{t}} = (h_{\mathrm{wind}} + h_{\mathrm{rg-sky}} + h_{\mathrm{cond1}})$$

In a similar way, the energy balance on the air flowing through the chimney results in the following equation:

$$h_{\mathrm{conv,g-a}} A_{\mathrm{g}} (T_{\mathrm{g}} - T_{\mathrm{f}}) + h_{\mathrm{conv,w-a}} A_{\mathrm{w}} (T_{\mathrm{w}} - T_{\mathrm{f}}) = q_{\mathrm{conv}} \quad (2)$$

where, $q_{\mathrm{conv}} = \dot{m} C_{\mathrm{p}} (T_{\mathrm{fo}} - T_{\mathrm{fi}})$

The average air temperature is calculated based on some sort of weighting between the air inlet, T_{fi}, and air exit, T_{fo}, of the chimney. This average temperature can be weighted as

$$T_{\mathrm{f}} = \omega T_{\mathrm{fo}} + (1 - \omega) T_{\mathrm{fi}}$$

where, ω (mean temperature weighting factor) was found in the literature to be 0.74 [4].

Consider the air inlet to the chimney has a temperature equal to the room average temperature, T_{r}, and substitute in the above equation of q_{conv} gives the following:

$$q_{\mathrm{conv}} = \dot{m} C_{\mathrm{p}} \frac{T_{\mathrm{f}} - T_{\mathrm{r}}}{\omega}$$

The absorber with its black surface and thermal mass is the main element in the chimney that mostly contributes to the energy carried by the moving air. The energy balance for this absorber is represented as follows:

$$\alpha_{\mathrm{w}} \tau_{\mathrm{g}} A_{\mathrm{w}} I = h_{\mathrm{rw-g}} A_{\mathrm{w}} (T_{\mathrm{w}} - T_{\mathrm{g}}) + h_{\mathrm{conv,w-a}} A_{\mathrm{w}} (T_{\mathrm{w}} - T_{\mathrm{f}}) + h_{\mathrm{cond-r}} A_{\mathrm{w}} (T_{\mathrm{w}} - T_{\mathrm{r}}) \quad (3)$$

The energy balance equations (1)–(3) can be reformulated into a matrix form as given below:

$$\begin{bmatrix} a_1 & b_1 & c_1 \\ a_2 & b_2 & c_2 \\ a_3 & b_3 & c_3 \end{bmatrix} \begin{Bmatrix} T_g \\ T_f \\ T_w \end{Bmatrix} = \begin{Bmatrix} R_1 \\ R_2 \\ R_3 \end{Bmatrix}$$

where, the matrix coefficients are defined as follows:

$$a_1 = h_{rw-g}A_w + h_{conv,g-a}Ag + (h_{wind} + h_{rg-sky} + h_{cond1})A_g,$$
$$b_1 = -h_{conv,g-a}A_g,\ c_1 = -h_{rw-g}A_w$$

$$a_2 = h_{conv,g-a}A_g,\ b_2 = -\left(h_{conv,g-a}A_g + h_{conv,w-a}A_w + \frac{\dot{m}C_p}{\omega}\right),$$

$$c_2 = h_{conv,w-a}A_w$$

$$a_3 = -h_{rw-g}A_w,\ b_3 = -h_{conv,w-a}A_w,$$
$$c_3 = h_{rw-g}A_w + h_{conv,w-a}A_w + h_{cond-r}A_w$$

The column vector terms in the right hand side of the matrix form are defined as

$$R_1 = \alpha_g A_g I + (h_{wind} + h_{cond1})A_g T_a + h_{rg-sky}A_g T_a, \quad R_2 = -\frac{\dot{m}C_p T_r}{\omega}$$

$$R_3 = \alpha_w \tau_g A_w I + h_{cond-r}A_w T_r$$

The above matrix is iteratively solved using the Gauss–Seidel method. Fig. 2 illustrates a graphical representation for the solution procedure. The solution starts with an initial guess for the unknown temperatures, T_g, T_f, and T_w. Then, the matrix is solved to obtain the converged temperatures. During solving for T_g at a present iteration, it takes into consideration the values of both T_f and T_w at previous iterations, while when solving for T_f, it depends on the value of T_g at the present iteration and T_w on a previous iteration. On the other hand, while solving for T_w, it considers both T_g and T_f values at the present iteration. Once the temperature values at a certain iteration are obtained, the flowing air properties as well as radiation and convection heat-transfer coefficients are updated based on these temperatures. These coefficients are as listed below [8,9]:

$h_{rw-g} = \frac{\sigma(T_w+T_g)(T_w^2+T_g^2)}{((1-\varepsilon_g)/\varepsilon_g)+((1-\varepsilon_w)/\varepsilon_w)+(1/F_{w-g})}$, where the shape factor, F_{w-g} is considered unity.

$$h_{rg-s} = \frac{\sigma\varepsilon_g(T_g + T_{sky})\left(T_g^2 + T_{sky}^2\right)(T_g - T_{sky})}{T_g - T_a}$$

Glass absorptivity was taken as 0.06 and transmitivity as 0.84; while the wall absorbitivity was 0.95. The sky temperature and wind coefficient can be calculated using [8]:

$$T_{sky} = 0.0552T_a^{1.5}, \quad \text{and} \quad h_{wind} = 2.8 + 3.0\upsilon_{wind}$$

The conduction heat-transfer coefficients for the glass and absorber walls are:

$$h_{cond1} = \frac{1}{(1/h_o) + (\Delta x_g/k_g)}, \quad h_{cond2} = \frac{1}{(1/h_i) + (\Delta x_{ins}/k_{ins})}$$

Air flowing in the chimney carries thermal energies from the glass and absorber walls by convection. So, the convective heat-transfer coefficients between air and both walls are:

$$h_{conv,g-a} = \frac{Nu\,k_{f\ @\ T_g}}{L_g}, \quad h_{conv,w-a} = \frac{Nu\,k_{f\ @\ T_w}}{L_w}$$

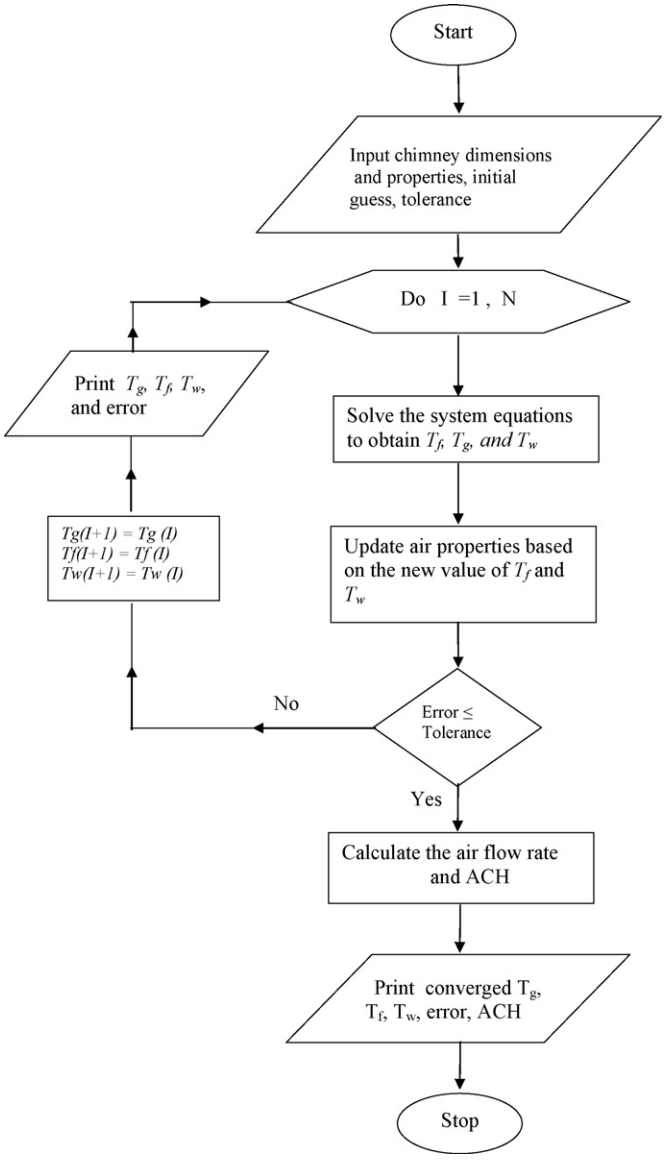

Fig. 2. A flow chart of the iterative procedure to solve the system matrix.

Once the converged temperatures are known, and the air properties are updated, the air flow rate can be calculated using the following relation [5]:

$$\dot{m} = \frac{C_d\rho_f A_o}{\sqrt{1 + (A_o^2/A_i^2)}}\sqrt{2gL_c\sin(\theta)\left[\frac{T_f}{T_r} - 1\right]}$$

The coefficient of discharge, C_d, is defined as the ratio of the cross-section area at the vena-contracta to the actual opening area. It was taken 0.57 due to the sharp edge inlet [4].

Since the main objective of the solar chimney is to enhance the natural ventilation in a space, it would be useful to know the variation of the ventilation rate, ACH, with the chimney inclination angle. The ratio of the air volume flow rate per hour divided by the space total volume defines the ACH.

Below are the correlations used to update the air properties based on the mean temperature defined as: $T_m = (T_f + T_s)/2$; where T_s stands for a surface average temperature. It is equal to T_g when the system is the glass wall, and equal to T_w when the

system is the absorber wall. These correlations are reported in [4] as

$$\beta = \frac{1}{T_m} \qquad \Delta T = T_s - T_f$$
$$\mu = (1.846 \times 10^{-5} + 0.00472 \times 10^{-5}(T_m - 300) \qquad k = 0.0263 + 0.000074(T_m - 300)$$
$$C_p = 1007 + 0.004(T_m - 300) \qquad \rho = 1.1614 - 0.00353(T_m - 300)$$
$$Pr = \frac{\mu C_p}{k}$$

The empirical relations for the Nusselt number are obtained from [9] for natural convection on inclined surfaces. For the range $10^{10} < Gr\,Pr < 10^{15}$, the following relations can be used:

$Nu = 0.17(Gr\,Pr)^{1/4}$, for turbulent flow and if the heated surface is facing upward, and $Nu = 0.17(Gr\cos^2\theta\,Pr)^{1/4}$ if the heated surface is facing downward.

Similarly, for laminar natural convection over an inclined surface, the relation becomes [9]:

$Nu = 0.6(Gr\cos\theta\,Pr)^{1/5}$ for $10^5 < Gr\,Pr < 10^{11}$, and constant wall heat flux.

In the present study, the value of $Gr\,Pr$, which is $g\beta\Delta TL^3/\upsilon\alpha$, varied from almost 3×10^9 to 5×10^9, hence the flow was treated laminar.

3. Numerical analysis

A commercial FEM-based code, Ansys, was used to predict the system flow pattern inside the space as a result of varying the inclination angle of the solar chimney. The main governing equations are the continuity, the y-momentum equation adopting the Boussinesq approximation of buoyancy force proportion to temperature difference, and the energy equation as follows [9]:

$$\frac{\partial u}{\partial x} + \frac{\partial v}{\partial y} = 0, \quad \left(u\frac{\partial u}{\partial x} + \upsilon\frac{\partial u}{\partial y}\right) = g\beta\beta(-T_\infty) + \nu\frac{\partial^2 u}{\partial y^2}, \quad \text{and} \quad \rho C_p\left(u\frac{\partial T}{\partial x} + \upsilon\frac{\partial T}{\partial y}\right) = k\frac{\partial^2 T}{\partial y^2}$$

The momentum equation and the energy equation were discretized using the finite element method. A quadrilateral element was chosen with a quadratic approximation of the velocity and temperature. The Galerkin principle is adopted for the weighted residual function. This helps constructing the element equation. An element assembly process was then carried out to connect elements together and impose the boundary conditions. These boundary conditions are as shown in Fig. 1(b). The global matrix is then iteratively solved over the computational domain shown in Fig. 1(b). Mesh refinement process is adopted in regions where sharp variation in the variable is expected, such as in the boundary layer regions. A Gradual mesh refinement was adopted to prove a grid independent solution. The eventual total number of elements was 3525 elements.

4. Results and discussion

The numerical flow prediction can be effectively used as an alternative procedure for flow visualization, particularly in the case of having difficulty to run experimental visualization. The inner flow pattern as a result of varying the chimney inclination angle was predicted and presented in Fig. 3 at different angles of: 15°, 30°, 45°, 60°, and 75°.

As can be noticed in Fig. 3, there is a noticeable effect of the chimney inclination angle on the space inlet flow penetration depth and pattern. The small inclination angle of 15° showed a high flow resistance at the chimney inlet due to the sudden flow contraction at the base of the chimney. This created a back pressure that resisted the inlet flow penetration depth. Once the absorber inclination angle increases to 30°, the flow starts to penetrate more through the window into the space, filling a larger portion of the space. The optimum flow pattern and penetration depth can be seen for inclination angles from 45° to 75°. Moreover, the figure showed that the flow covers most of the space area including the occupied zone (1.8 m above the floor) in this angle range, which is not seen for angles below 45°.

The temperature variation of the glass wall, air, and absorber wall was calculated using a FORTRAN computer program that was developed based on the general relaxation iterative method considering the relaxation factor to be unity. Fig. 2 shows a general representation of the program sequential processes.

The variation of temperatures at different solar intensities for an inclination angle of 45° was presented and compared with analytical and experimental results published by Mathur et al. [4]. This comparison, shown in Fig. 4, validates both the numerical as well as the analytical results. As the figure indicates, all temperatures gradually increase as the solar intensity increases and reach a nearly asymptotic behavior. It can be also seen that the absorber posses a high temperature value compared to the glass and air temperatures. This increase in absorber temperature is due to capturing more radiation as a result of its black surface nature and storing high thermal energy. In addition, its reflectivity and transmitivity are almost zero.

The variation of air exit velocity is dependent on the absorber inclination angle. Fig. 5 illustrates that the air exit velocity increases as the inclination angle with the horizontal plane increases. The velocity reaches its maximum value almost beyond 45°. This exit velocity will help entraining more fresh air to the space from outdoor. A comparison of the predicted exit velocity at latitude of 28.4° is shown with that presented in [5] at latitude of 40.07°. Both trends indicate the velocity increase as the inclination angle increases to an optimum range corresponding to 45° to 75°. Although the radiation captured by the absorber decreases as the inclination angle increases, but the "stack height" ($L\sin\theta$) increases and becomes of dominant effect on the exist velocity. This enhanced the exit velocity and accordingly the space ACH. Moreover, at a small inclination angle both trends showed almost close exit velocity values. This can be explained by the high flow resistance at the chimney inlet due to the sudden contraction obstructing the flow into the chimney. On the other side, as the inclination angle increases, these inlet losses decrease allowing the flow to be entrained into the chimney. The discrepancy

Table 1
Comparing the air flow rate at different solar intensities

Intensity (W/sq.m)	Air flow rate (kg/min) at an inclination angle 45°		
	Theo. [4]	Exp. [4]	Present
500	3.735	4.275	3.388
550	3.833	4.521	3.514
600	3.956	4.521	3.627
650	4.029	4.865	3.735
700	4.226	5.233	3.833
750	4.324	5.405	3.939

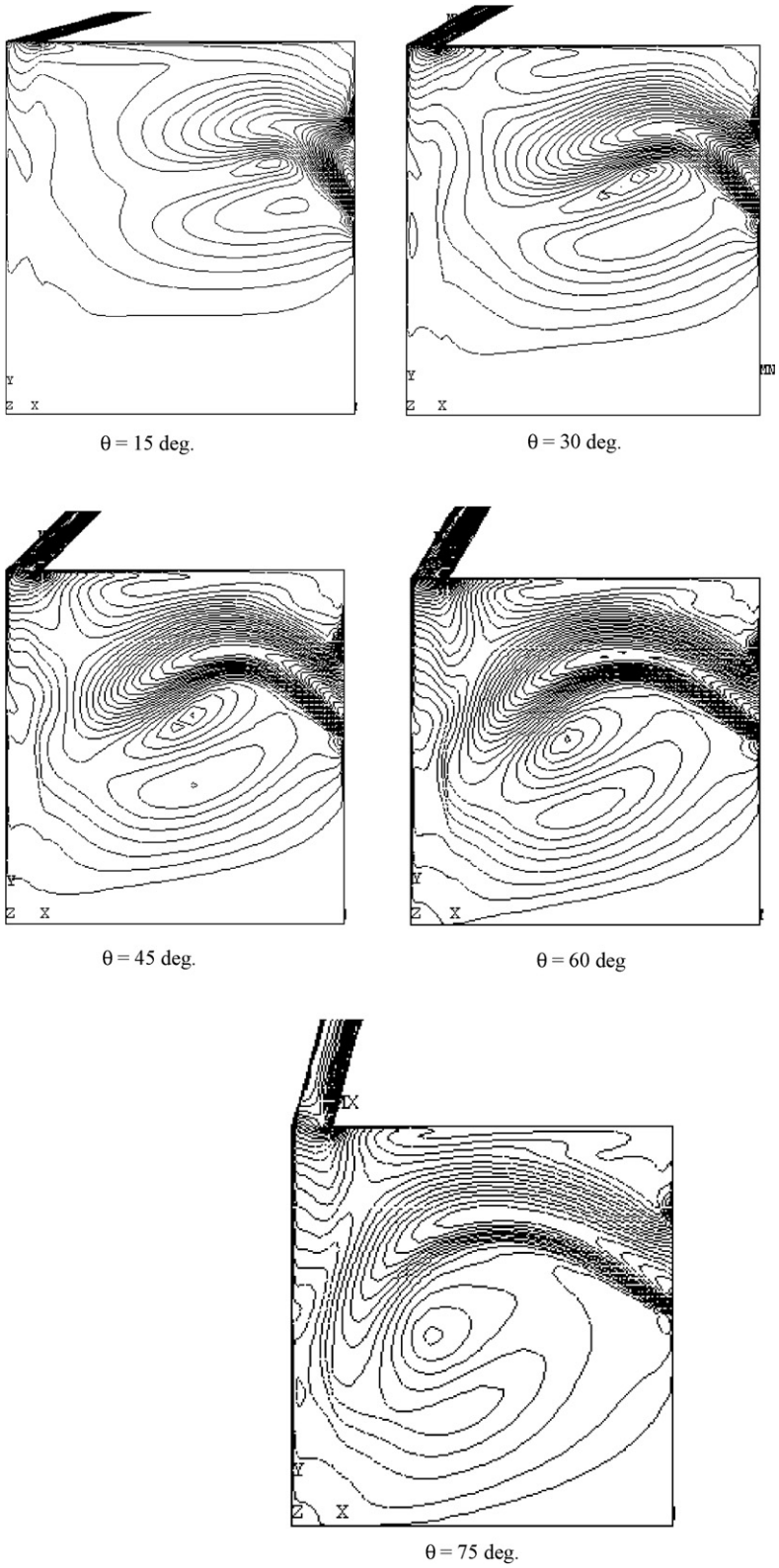

Fig. 3. Space flow pattern variation with inclination angles.

between both trends is due to the gap width variation. In addition, it can be concluded from the figure that the chimney gap width could have a minor effect on the air exit velocity at inclination angles below 20°.

Table 1 summarizes a quantitative comparison for the air flow rate passing through the chimney at an inclination angle of 45° at different solar intensities. The comparison was held with Mathur et al. [4] whose results were for a chimney width of 0.35 m and latitude of 27°, similar to our conditions that are: 0.35 m for a chimney width, and latitude of 28.4°. The table indicates that both theoretical predictions underpredicted the air flow rate by nearly 20%. However, the values showed the improvement of the air flow

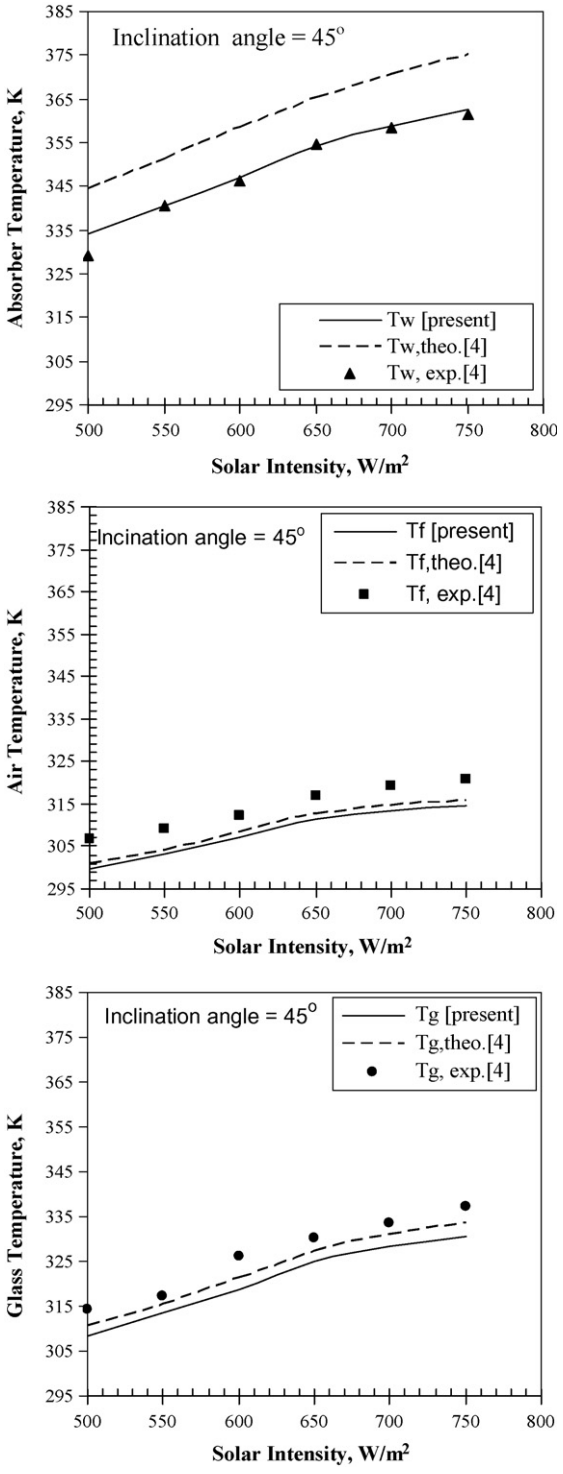

Fig. 4. Temperature variation with solar intensity for 45° inclination angle.

rate as the solar intensity increases. This is related to the more energy absorbance by the absorber.

For the studied configuration, a correlation was sought to relate the ACH to both solar intensity (I), chimney width (d), and inclination angle (θ). It was found from manipulating the results that a correlation in the form of: $ACH = 0.795(\sin(\theta)^{0.3189} I^{0.3818} d^{0.1658})$ can be used to predict the ACH. The correlation was tested within a solar

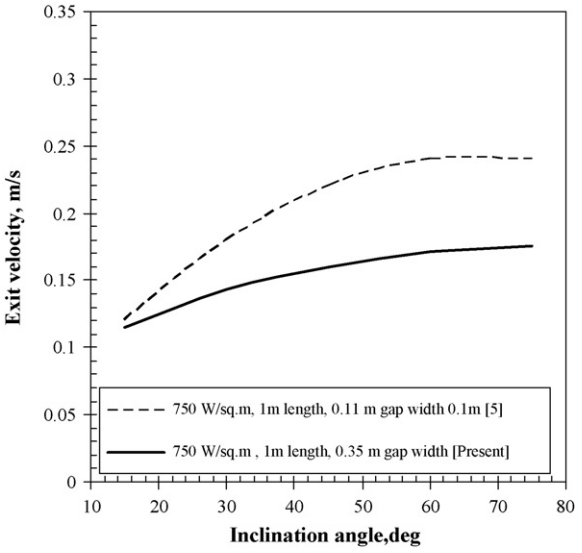

Fig. 5. Chimney air exit velocity variation with inclination angle.

intensity greater than or equal to 500 W/m^2, and chimney width from 0.1 m to 0.35 m for different inclination angles with acceptable values.

5. Conclusions

The present study aimed at investigating the effect of solar chimney inclination angle on ventilation rate and space flow pattern. Out of the results, the following can be drawn:

1. A distinct effect of the inclination angle on the space flow pattern was found insuring an optimum inclination range between 45° and 75° with latitude of 28.4°.
2. The numerical visualization of space flow pattern showed the increase of space inlet flow penetration depth as the inclination angle increases.
3. The air change per hour can be roughly estimated based on a concluded correlation in the form: $ACH = 0.795(\sin(\theta)^{0.3189} I^{0.3818} d^{0.1658})$, with an error of 20% approximately under the following limitations: intensity $\geq$500 W/m^2, air gap width from 0.1 m to 0.35 m.

References

[1] B. Ramadan, K. Nader, An analytical and numerical study of solar chimney use for room natural ventilation, Energy and Buildings 40 (2008) 865–873.
[2] C. Sudaporn, L. Bundit, Application of passive cooling systems in the hot and humid climate: the case study of solar chimney and wetted roof in Thailand, Building and Environment 42 (2007) 3341–3351.
[3] J. Mathur, Anupma, S. Mathur, Experimental investigation on four different types of solar chimneys, Advances in Energy Research (2006) 151–156.
[4] J. Mathur, S. Mathur, Anupma, Summer-performance of inclined roof solar chimney for natural ventilation, Energy and Buildings 38 (2006) 1156–1163.
[5] E. Sakonidou, T. Karapantsios, A. Balouktsis, D. Chassapis, Modeling of the optimum tilt of a solar chimney for maximum air flow, Solar Energy 82 (2008) 80–94.
[6] C. Tawit, T. Pornsawan, Natural ventilation in building using attic and solar chimney, in: The Joint International Conference on Sustainable Energy and Environment (SEE), Hua Hin, Thailand, (2004), pp. 45–48.
[7] D.J. Harris, N. Helwig, Solar chimney and building ventilation, Applied Energy 84 (2007) 135–146.
[8] J.A. Duffie, W.A. Beckman, Solar Energy Thermal processes, John Wiley and Sons Inc., 1974.
[9] J.P. Holman, Heat Transfer, 5th edition, McGraw-Hill Co., 1981.